EUROPEAN ORGANIZATION FOR NUCLEAR RESEARCH

CERN-EP/98-156
10 October 1998

# Measurement of the $e^+e^- \rightarrow Z \rightarrow b\bar{b}$ Forward-Backward Asymmetry and the $B^0\bar{B}^0$ Mixing Parameter Using Prompt Leptons

The L3 Collaboration

## Abstract

The time-integrated $B^0\bar{B}^0$ mixing parameter and the forward-backward charge asymmetry in the process $e^+e^- \rightarrow b\bar{b}$ are measured in hadronic Z events containing prompt muons or electrons, collected by the L3 experiment in the years 1990 to 1995. The total sample of 3.3 million hadronic Z events with a mean centre-of-mass energy of 91.26 GeV yields:

$$\begin{aligned} A_{FB}^{b} &= 0.0960 \pm 0.0066(stat.) \pm 0.0033(sys.)\,, \\ \chi_b &= 0.1192 \pm 0.0068(stat.) \pm 0.0051(sys.)\,. \end{aligned}$$

This asymmetry measurement together with measurements at energies away from the Z pole energy yield a pole asymmetry and corresponding effective electroweak mixing angle of:

$$\begin{aligned} A_{FB}^{0,b} &= 0.1015 \pm 0.0064(stat.) \pm 0.0035(sys.)\,, \\ \sin^2\bar{\theta}_W &= 0.2318 \pm 0.0013\,. \end{aligned}$$

Submitted to *Phys. Lett. B*

# Introduction

In the process $e^+e^- \to Z \to b\bar{b}$ , the distribution of the quark production angle $\theta_b$ relative to the electron beam direction can be parametrised by:

$$\frac{d\sigma}{d\cos\theta_b} \propto \frac{3}{8}(1+\cos^2\theta_b) + A_{FB}^b \cos\theta_b.$$

Within the Standard Model [1] for lowest order Z exchange, at $\sqrt{s} = m_Z$, the forward-backward pole asymmetry $A_{FB}^{0,b}$ is related to the vector $v_f$ and axial-vector $a_f$ couplings of fermions to the Z boson by:

$$A_{FB}^{0,b} = \frac{3}{4}\frac{2v_e a_e}{v_e^2 + a_e^2}\frac{2v_b a_b}{v_b^2 + a_b^2}. \quad (1)$$

Higher order corrections are accounted for by replacing the couplings $v_f$,$a_f$ with modified effective couplings $\bar{v}_f$,$\bar{a}_f$ [2] which are related by:

$$\frac{\bar{v}_f}{\bar{a}_f} = 1 - 4|q_f|\sin^2\bar{\theta}_W, \quad (2)$$

where $q_f$ is the fermion charge and $\bar{\theta}_W$ is the effective electroweak mixing angle.

The high sensitivity of the down type quark asymmetries to $\sin^2\bar{\theta}_W$ and the relative ease of selecting pure $Z \to b\bar{b}$ samples make $A_{FB}^b$ measurements excellent tests of Standard Model predictions.

Due to mixing in the $B^0\bar{B}^0$ system where a $B_d^0$ or $B_s^0$ oscillates into its anti-particle the observed asymmetry is diluted by a factor $1/(1-2\chi_b)$, where $\chi_b$ is the mixing parameter. In the Standard Model the oscillation proceeds by a weak flavour-changing box diagram, dominated by virtual top-quark exchange. The rate of mixing depends on the Cabibbo-Kobayashi-Maskawa matrix elements, $V_{td}$ and $V_{ts}$, the top-quark mass and the B meson decay constant.

Electrons and muons from the semileptonic decays of b-quarks are used to select events coming from $Z \to b\bar{b}$. The large mass and hard fragmentation of the b-quark results in prompt leptons from b-quark decays having high momentum $p$ and transverse momentum $p_t$ with respect to the quark direction; the $p_t$ reflects the momentum distribution in the centre-of-mass frame of the heavy hadron. Thus, a high $p, p_t$ lepton within a jet provides both b-flavour enhancement and charge information, from the correlation of the lepton charge, $q$, with the quark charge. The quark direction estimator is obtained from the event thrust axis. Prompt leptons constitute roughly 1% of all charged particles produced in hadronic events. Thus, both effective background rejection and lepton selection are required.

Events containing two high $p, p_t$ leptons in different jets allow the rate of mixing to be determined. As both oscillations from $B_d^0$ and $B_s^0$ mesons contribute to the observed mixing, $\chi_b = f_d\chi_d + f_s\chi_s$, where $f_d$ and $f_s$ are the production fractions of $B_d^0$ and $B_s^0$ mesons.

In this paper, measurements of $A_{FB}^b$ and $\chi_b$ with the L3 detector [3], using events collected at centre-of-mass energies, $\sqrt{s}$, close to the Z pole energy during the data taking periods of 1993-1995, are presented. The data sample consists of 2.3 million hadronic events with mean energy 91.24 GeV. Measurements using data collected during 1993-1995 at centre-of-mass energies significantly below and above the pole energy are also presented. These measurements are combined with previous L3 results [4] using data from the 1990-1992 running periods, corresponding to 1.04 million hadronic events. The combined result is used to extract a value for the effective weak mixing angle $\sin^2\bar{\theta}_W$ . Other LEP measurements of these quantities are reported in References [5–8].

## Event selection

A detailed description of the L3 detector is provided by Reference [3]. The trigger requirements and the selection criteria for hadronic events containing electrons or muons have been described previously [9,10]. Muons are identified and measured in the muon chamber system. We require that a muon track consists of track segments in at least two of the three layers of muon chambers, and that the muon track points back to the interaction region. Electrons are identified using the electromagnetic and hadronic calorimeters, as well as the central tracking chamber. Only electrons in the barrel region $|\cos\theta| < 0.69$ are considered for this analysis. Requiring less than 3 GeV to be deposited in a cone of half angle $7^\circ$ behind the electromagnetic cluster rejects hadrons which fulfil the electron shower shape and energy criteria in the electromagnetic calorimeter. Photons are rejected by requiring a track in the central tracking chamber to be matched with the electromagnetic cluster. The track curvature in the central tracking chamber determines the charge of the electron. The electron selection, in particular the shower shape criteria, implies an isolation requirement on identified electrons. This results in a lower efficiency for electrons than for muons.

The momentum of muon candidates is required to be greater than 4 GeV, while the electron candidates are required to have momentum greater than 3 GeV. Requirements on the transverse momentum $p_t > 1$ GeV of the leptons are used to further enhance the $\mathrm{b\bar{b}}$ purity. The transverse momentum is defined with respect to the nearest jet, where the measured momentum of the lepton is excluded from the jet. If there is no jet with an energy greater than 6 GeV in the same hemisphere as the lepton, the $p_t$ is calculated relative to the thrust axis of the event. In events containing more than one lepton candidate, only the highest $p_t$ lepton is used in the asymmetry analysis.

For the mixing determination, two leptons are required with a separation angle of more than $60^\circ$ to provide tagging information from two b-hadrons originating from different jets. The transverse momenta of the leptons are required to be greater than 0.5 GeV. In events containing more than two leptons the two with the highest transverse momentum are considered.

After hadron selection and detector quality requirements the total number of hadronic events selected is 2.3 million, at a mean centre-of-mass energy of 91.24 GeV. Of these, the number with prompt lepton candidates selected is 79417, comprising 55597 with muon candidates and 23820 with electron candidates. The number of dilepton events selected, after all cuts is 4452, comprising 2046 muon-muon candidates, 1874 muon-electron candidates and 532 electron-electron candidates.

## Event simulation

The JETSET 7.4 Monte Carlo program [11] is used to generate event samples, simulating the fragmentation and decay of hadronic events. The events are passed through the full L3 detector simulation [12], which includes the effects of experimental resolution, energy loss, multiple scattering, interactions and decays in the detector materials.

Relevant electroweak parameters, fragmentation parameters, semileptonic decay models, and branching ratios are set to their current best values and the uncertainties on these parameters are used to determine the systematic uncertainties on the results. The parameter values and variations follow the recommendations developed in Reference [13] and updated in Reference [14]; and are summarised below together with the resulting systematic uncertainties on $A_{\mathrm{FB}}^{\mathrm{b}}$ and $\chi_{\mathrm{b}}$ .

The distributions of the scaled energy ($x_{\mathrm{E}} = 2E_{\mathrm{hadron}}/\sqrt{s}$) of weakly decaying heavy hadrons are modelled using the Peterson fragmentation function [15]. The shape determining Peterson parameters $\epsilon_{\mathrm{b}}$,$\epsilon_{\mathrm{c}}$ for b and c hadrons are adjusted to attain the recommended mean scaled energies $\langle x_{\mathrm{E}}(\mathrm{b})\rangle$ and $\langle x_{\mathrm{E}}(\mathrm{c})\rangle$ . The lepton momentum spectra implemented in JETSET are re-weighted using several models, adjusting the spectra for both the 'central point' at which the measurement is made as well as the 'upper' and 'lower' points used to determine the systematic uncertainties. The sign convention used is for the harder and softer spectra to be modelled by the upper and lower points, respectively. For $\mathrm{b} \rightarrow \ell$ decays the ACCMM model [16] with Fermi momentum $p_{\mathrm{f}} = 298$ MeV and produced c-quark mass 1673 MeV is used as the central point, and the ISGW model [17] with 11% $\mathrm{D}^{**}$ and 32% $\mathrm{D}^{**}$ (ISGW$^{**}$) are used as upper and lower points of the systematic variation. For $\mathrm{c} \rightarrow \ell$ decays the ACCMM model is used as a convenient functional form, with parameters for the central point and variations chosen from fits to DELCO [18] and MARK III [19] data. For the $\mathrm{b} \rightarrow \mathrm{c} \rightarrow \ell$ decay chain, the $\mathrm{b} \rightarrow \mathrm{D}$ spectrum measured by CLEO [20] is combined with the $\mathrm{c} \rightarrow \ell$ spectrum corrected by the procedure described above.

Monte Carlo events with single leptons, or the highest $p_t$ lepton in multi-lepton events, are classified into six categories: $\mathrm{b} \rightarrow \ell$, $\mathrm{b} \rightarrow \mathrm{c} \rightarrow \ell$, $\mathrm{b} \rightarrow \tau \rightarrow \ell$, $\mathrm{b} \rightarrow \bar{\mathrm{c}} \rightarrow \ell$, $\mathrm{c} \rightarrow \ell$ and background. Where the class $\mathrm{b} \rightarrow \bar{\mathrm{c}} \rightarrow \ell$ represents the cascade $\mathrm{b} \rightarrow \mathrm{W} \rightarrow \bar{\mathrm{c}} \rightarrow \ell$. The background includes leptons from $\pi$ and K decays, Dalitz decays, photon conversions and misidentified hadrons. Examples of the causes of misidentifying hadrons as leptons are $\pi - \gamma$ overlaps for electrons and punchthrough for muons. The Monte Carlo estimate of the sample composition is shown in Table 1 together with the asymmetry contribution of each source.

Simulated events with two leptons separated by more than 60° are classified into eight categories, listed in Table 2 together with the estimated sample composition.

# Asymmetry Determination

The observed asymmetry is extracted by applying an event by event unbinned maximum-likelihood fit to the $p$ and $p_t$ distributions, assuming no $\mathrm{B}^0\bar{\mathrm{B}}^0$ mixing. The likelihood function has the form:

$$\mathcal{L} = \prod_{i=1}^{N_{\mathrm{data}}} \sum_{k=1}^{6} f_k(i) \cdot [\frac{3}{8}(1+\cos^2\theta_i) + A_k \, \cos\theta_i].$$

For each data lepton $i$ the fractions in each category $k$, $f_k(i)$, are determined from the number and type of Monte Carlo leptons found within a rectangular box centered on the data lepton in the $p$-$p_t$ plane. The box dimensions are increased until a minimum of 30 Monte Carlo leptons are included in the box. The six categories are listed in Table 1 together with their associated asymmetries $A_k$, which parameterise the angular distributions for each of the classes. The asymmetries $A_k$ enter the likelihood function in the bracketed weighting factor; only $A_b$ is left free in the fit. The estimate of the b-quark direction $\cos\theta_i$ is obtained from the observable $-q\,\cos\theta_{\mathrm{T}}$, where the thrust direction $\theta_{\mathrm{T}}$ is oriented into the hemisphere containing the lepton, of charge $q$. Figures 1 and 2 show the $p$, $p_t$ and $-q\,\cos\theta_{\mathrm{T}}$ distributions for the selected electrons and muons together with the predicted Monte Carlo fractions of the various sources. While the $p$,$p_t$ distributions for the various classes are the principal Monte Carlo inputs to the asymmetry fit, it is also important that no asymmetry in $-q\,\cos\theta_{\mathrm{T}}$ is introduced by detector effects. No such detector introduced asymmetry has been observed and tolerable agreement is seen in all the distributions.

## Extraction of the Mixing Parameter

A maximum-likelihood fit, described in detail in Reference [10], is used to extract the mixing parameter. The probability functions for the two leptons to come from various sources are assumed to factorize, allowing the functions to be determined independently from single lepton Monte Carlo events by counting the number and type of Monte Carlo leptons found in $(p_l, p_t)$ boxes, where $p_l$ is the lepton momentum along the jet axis.

A global probability function, with terms representing each of the different sign combinations of the two leptons, is constructed from the single lepton probability functions and several parameters, namely $\alpha$, which is the fraction of $\mathrm{b\bar{b}}$ events in the dilepton sample, $\beta$, the fraction of (u,d,s,c) with opposite charges in the dilepton sample, $B$, the fraction of $\mathrm{b} \rightarrow \ell$ events in the total b decay sample and $C(p_1, p_2)$ which takes into account possible correlations between the lepton momenta.

Parameters $\alpha$, $\beta$ and $B$ are evaluated from the Monte Carlo sample and are fixed in the fit ($\alpha = 0.813$, $\beta = 0.070$, $B = 0.705$). The contribution of these parameters to the systematic uncertainties are evaluated by a 2 % variation around the fixed values, corresponding to the estimated error on the value. As Monte Carlo studies have shown that the correlation parameter $C$ is compatible with zero, it is fixed at zero in the fit.

Figure 3 shows the stability of $\chi_\mathrm{b}$ as a function of the minimum transverse momentum of the two leptons. Results from the maximum-likelihood fit are compared with results from a simple counting method [10], used as a cross-check.

## Results

The $A_\mathrm{FB}^\mathrm{b}$ results from the 1993-1995 data sample at the Z peak, with an average centre-of-mass energy of 91.24 GeV, and the $\chi_\mathrm{b}$ results from all energy points are:

$$\begin{aligned} A_\mathrm{FB}^\mathrm{b} &= 0.0977 \pm 0.0080(stat.) \pm 0.0033(sys.) \\ \chi_\mathrm{b} &= 0.1172 \pm 0.0083(stat.) \pm 0.0051(sys.) \end{aligned}$$

The observed asymmetry is corrected for the effects of mixing using the reported $\chi_\mathrm{b}$ value and the $A_\mathrm{FB}^\mathrm{b}$ uncertainties take account of correlations between the systematics of the mixing and observed asymmetry determinations.

Details of the systematic uncertainties are provided in Table 3, including dependencies on other electroweak parameters; the parameter values and variations are listed. The electroweak parameters varied include the ratios of the b and c quark partial widths of the Z to its total hadronic partial width, $R_b$ and $R_c$ , as well as the forward-backward asymmetry of c quarks, $A_\mathrm{FB}^\mathrm{c}$ ; the values and variations used correspond to the world average results reported in Reference [21]. Separate fits for muons and electrons are performed, yielding the statistically consistent results $0.103 \pm 0.009$ and $0.088 \pm 0.014$ respectively. Estimates of the charge confusion for muons and electrons are made and corrections are applied. The error on the charge confusion estimate is included as a contribution to the systematic error.

Effects of reconstruction uncertainties in the simulation of the lepton momentum and in the jet direction determination are estimated by smearing the lepton momentum by 2% and the angle between the lepton and the nearest jet by 1°. Monte Carlo studies show the background asymmetry to be consistent with zero, we vary this by $\pm 0.01$ as an estimate of the uncertainty on this quantity.

The results for $A_{\rm FB}^{\rm b}$ , from the peak data alone, and $\chi_{\rm b}$ are combined with the 1990-1992 results [4] to yield:

$$\begin{aligned} A_{\rm FB}^{\rm b} &= 0.0960 \pm 0.0066(stat.) \pm 0.0033(sys.) \\ \chi_{\rm b} &= 0.1192 \pm 0.0068(stat.) \pm 0.0051(sys.) \end{aligned}$$

from the total sample of 3.3 million hadronic Z decays. The data is divided into energies below, on and above the Z resonance due to the centre-of-mass energy dependence of $A_{\rm FB}^{\rm b}$ , as illustrated in Table 4 and Figure 4. The results after applying QCD corrections, to remove the diluting effects of QCD, are compared with the Standard Model predictions of ZFITTER [22] with QCD effects removed. The Standard Model parameters used correspond to $\sin^2\bar{\theta}_{\rm W} = 0.2315$. In performing the combination it was necessary to re-evaluate some systematic uncertainties from the 1990-92 analysis to account for significant non-linear behaviour of the uncertainties as a function of the input parameters, particularly for $\mathrm{Br}(\mathrm{b}\to\ell)$.

# Determination of $\sin^2\bar{\theta}_{\rm W}$

In order to convert the three measured asymmetries $A_{\rm FB}^{\rm b}$ to a pole asymmetry $A_{\rm FB}^{0,\rm b}$ or equivalently $\sin^2\bar{\theta}_{\rm W}$ , corrections to account for the centre-of-mass energy dependence are applied to the off-peak points, allowing a combination with the peak point. Further small corrections are applied to account for QED and QCD effects as well as effects from the centre-of-mass energy dependence, as described in Reference [13]. The event selection bias $s_b$ and QCD correction factor $C_b$, defined by:

$$A_{\rm FB}^{\rm b} = (1 - s_b \times \delta_{\rm QCD,ref}^{\rm had,T}) A_{\rm FB}^{0,\rm b} = (1 - C_b) A_{\rm FB}^{0,\rm b}\,,$$

are obtained from Monte Carlo and generator level studies to be $s_b = 0.72 \pm 0.12(stat.)$ and $C_b = (2.07 \pm 0.36(stat.) \pm 0.24(th.))\%$ , where the reference value $\delta_{\rm QCD,ref}^{\rm had,T}$ is determined to be $(2.87 \pm 0.35)\%$ using the results of analytic calculations at parton level corrected by generator studies of the effects of hadronisation. Full details of the determination of the QCD correction applied to this analysis are provided in Reference [23].

Equations 1 and 2 are used to relate the pole asymmetry $A_{\rm FB}^{0,\rm b}$ to $\sin^2\bar{\theta}_{\rm W}$ , yielding results from the full 1990-1995 data sample:

$$\begin{aligned} A_{\rm FB}^{0,\rm b} &= 0.1015 \pm 0.0064(stat.) \pm 0.0035(sys.)\,, \\ \sin^2\bar{\theta}_{\rm W} &= 0.2318 \pm 0.0013\,. \end{aligned}$$

The results are compatible with previous L3 and LEP measurements, and are consistent with Standard Model expectations.

# Acknowledgments

We wish to express our gratitude to the CERN accelerator divisions for the excellent performance of the LEP machine. We acknowledge the contributions of all the engineers and technicians who have participated in the construction and maintenance of this experiment.

## The L3 Collaboration:


M.Acciarri,[27] P.Achard,[19] O.Adriani,[16] M.Aguilar-Benitez,[26] J.Alcaraz,[26] G.Alemanni,[22] J.Allaby,[17] A.Aloisio,[29] M.G.Alviggi,[29] G.Ambrosi,[19] H.Anderhub,[48] V.P.Andreev,[7,37] T.Angelescu,[13] F.Anselmo,[10] A.Arefiev,[28] T.Azemoon,[3] T.Aziz,[11] P.Bagnaia,[36] L.Baksay,[43] A.Balandras,[4] R.C.Ball,[3] S.Banerjee,[11] Sw.Banerjee,[11] K.Banicz,[45] A.Barczyk,[48,46] R.Barillère,[17] L.Barone,[36] P.Bartalini,[22] M.Basile,[10] R.Battiston,[33] A.Bay,[22] F.Becattini,[16] U.Becker,[15] F.Behner,[48] J.Berdugo,[26] P.Berges,[15] B.Bertucci,[33] B.L.Betev,[48] S.Bhattacharya,[11] M.Biasini,[33] A.Biland,[48] G.M.Bilei,[33] J.J.Blaising,[4] S.C.Blyth,[34] G.J.Bobbink,[2] R.Bock,[1] A.Böhm,[1] L.Boldizsar,[14] B.Borgia,[17,36] D.Bourilkov,[48] M.Bourquin,[19] S.Braccini,[19] J.G.Branson,[39] V.Brigljevic,[48] F.Brochu,[4] I.C.Brock,[34] A.Buffini,[16] A.Buijs,[44] J.D.Burger,[15] W.J.Burger,[33] J.Busenitz,[43] A.Button,[3] X.D.Cai,[15] M.Campanelli,[48] M.Capell,[15] G.Cara Romeo,[10] G.Carlino,[29] A.M.Cartacci,[16] J.Casaus,[26] G.Castellini,[16] F.Cavallari,[36] N.Cavallo,[29] C.Cecchi,[19] M.Cerrada,[26] F.Cesaroni,[23] M.Chamizo,[26] Y.H.Chang,[50] U.K.Chaturvedi,[18] M.Chemarin,[25] A.Chen,[50] G.Chen,[8] G.M.Chen,[8] H.F.Chen,[20] H.S.Chen,[8] X.Chereau,[4] G.Chiefari,[29] L.Cifarelli,[38] F.Cindolo,[10] C.Civinini,[16] I.Clare,[15] R.Clare,[15] G.Coignet,[4] A.P.Colijn,[2] N.Colino,[26] S.Costantini,[9] F.Cotorobai,[13] B.de la Cruz,[26] A.Csilling,[14] T.S.Dai,[15] J.A.van Dalen,[31] R.D'Alessandro,[16] R.de Asmundis,[29] P.Deglon,[19] A.Degré,[4] K.Deiters,[46] D.della Volpe,[29] P.Denes,[35] F.DeNotaristefani,[36] A.De Salvo,[48] M.Diemoz,[36] D.van Dierendonck,[2] F.Di Lodovico,[48] C.Dionisi,[17,36] M.Dittmar,[48] A.Dominguez,[39] A.Doria,[29] M.T.Dova,[18,♯] D.Duchesneau,[4] D.Dufournand,[4] P.Duinker,[2] I.Duran,[40] S.Easo,[33] H.El Mamouni,[25] A.Engler,[34] F.J.Eppling,[15] F.C.Erné,[2] P.Extermann,[19] M.Fabre,[46] R.Faccini,[36] M.A.Falagan,[26] S.Falciano,[36] A.Favara,[16] J.Fay,[25] O.Fedin,[37] M.Felcini,[48] T.Ferguson,[34] F.Ferroni,[36] H.Fesefeldt,[1] E.Fiandrini,[33] J.H.Field,[19] F.Filthaut,[17] P.H.Fisher,[15] I.Fisk,[39] G.Forconi,[15] L.Fredj,[19] K.Freudenreich,[48] C.Furetta,[27] Yu.Galaktionov,[28,15] S.N.Ganguli,[11] P.Garcia-Abia,[6] M.Gataullin,[32] S.S.Gau,[12] S.Gentile,[36] N.Gheordanescu,[13] S.Giagu,[36] S.Goldfarb,[22] Z.F.Gong,[20] G.Gratta,[32] M.W.Gruenewald,[9] R.van Gulik,[2] V.K.Gupta,[35] A.Gurtu,[11] L.J.Gutay,[45] D.Haas,[6] B.Hartmann,[1] A.Hasan,[30] D.Hatzifotiadou,[10] T.Hebbeker,[9] A.Hervé,[17] P.Hidas,[14] J.Hirschfelder,[34] H.Hofer,[48] G. Holzner,[48] H.Hoorani,[34] S.R.Hou,[50] I.Iashvili,[47] B.N.Jin,[8] L.W.Jones,[3] P.de Jong,[17] I.Josa-Mutuberría,[26] A.Kasser,[22] R.A.Khan,[18] D.Kamrad,[47] J.S.Kapustinsky,[24] M.Kaur,[18,◇] M.N.Kienzle-Focacci,[19] D.Kim,[36] D.H.Kim,[42] J.K.Kim,[42] S.C.Kim,[42] W.W.Kinnison,[24] A.Kirkby,[32] D.Kirkby,[32] J.Kirkby,[17] D.Kiss,[14] W.Kittel,[31] A.Klimentov,[15,28] A.C.König,[31] A.Kopp,[47] I.Korolko,[28] V.Koutsenko,[15,28] R.W.Kraemer,[34] W.Krenz,[1] A.Kunin,[15,28] P.Lacentre,[47,♮,♯] P.Ladron de Guevara,[26] I.Laktineh,[25] G.Landi,[16] C.Lapoint,[15] K.Lassila-Perini,[48] P.Laurikainen,[21] A.Lavorato,[38] M.Lebeau,[17] A.Lebedev,[15] P.Lebrun,[25] P.Lecomte,[48] P.Lecoq,[17] P.Le Coultre,[48] H.J.Lee,[9] J.M.Le Goff,[17] R.Leiste,[47] E.Leonardi,[36] P.Levtchenko,[37] C.Li,[20] C.H.Lin,[50] W.T.Lin,[50] F.L.Linde,[2,17] L.Lista,[29] Z.A.Liu,[8] W.Lohmann,[47] E.Longo,[36] W.Lu,[32] Y.S.Lu,[8] K.Lübelsmeyer,[1] C.Luci,[17,36] D.Luckey,[15] L.Luminari,[36] W.Lustermann,[48] W.G.Ma,[20] M.Maity,[11] G.Majumder,[11] L.Malgeri,[17] A.Malinin,[28] C.Maña,[26] D.Mangeol,[31] P.Marchesini,[48] G.Marian,[43,¶] J.P.Martin,[25] F.Marzano,[36] G.G.G.Massaro,[2] K.Mazumdar,[11] R.R.McNeil,[7] S.Mele,[17] L.Merola,[29] M.Meschini,[16] W.J.Metzger,[31] M.von der Mey,[1] Y.Mi,[22] D.Migani,[10] A.Mihul,[13] H.Milcent,[17] G.Mirabelli,[36] J.Mnich,[17] P.Molnar,[9] B.Monteleoni,[16] T.Moulik,[11] R.Mount,[32] G.S.Muanza,[25] F.Muheim,[19] A.J.M.Muijs,[2] S.Nahn,[15] M.Napolitano,[29] F.Nessi-Tedaldi,[48] H.Newman,[32] T.Niessen,[1] A.Nippe,[22] A.Nisati,[36] H.Nowak,[47] Y.D.Oh,[42] G.Organtini,[36] R.Ostonen,[21] C.Palomares,[26] D.Pandoulas,[1] S.Paoletti,[36,17] P.Paolucci,[29] H.K.Park,[34] I.H.Park,[42] G.Pascale,[36] G.Passaleva,[17] S.Patricelli,[29] T.Paul,[12] M.Pauluzzi,[33] C.Paus,[17] F.Pauss,[48] D.Peach,[17] M.Pedace,[36] Y.J.Pei,[1] S.Pensotti,[27] D.Perret-Gallix,[4] B.Petersen,[31] S.Petrak,[9] A.Pevsner,[5] D.Piccolo,[29] M.Pieri,[16] P.A.Piroué,[35] E.Pistolesi,[27] V.Plyaskin,[28] M.Pohl,[48] V.Pojidaev,[28,16] H.Postema,[15] J.Pothier,[17] N.Produit,[19] D.Prokofiev,[37] J.Quartieri,[38] G.Rahal-Callot,[48] N.Raja,[11] P.G.Rancoita,[27] M.Rattaggi,[27] G.Raven,[39] P.Razis,[30] D.Ren,[48] M.Rescigno,[36] S.Reucroft,[12] T.van Rhee,[44] S.Riemann,[47] K.Riles,[3] A.Robohm,[48] J.Rodin,[43] B.P.Roe,[3] L.Romero,[26] S.Rosier-Lees,[4] Ph.Rosselet,[22] S.Roth,[1] J.A.Rubio,[17] D.Ruschmeier,[9] H.Rykaczewski,[48] S.Sakar,[36] J.Salicio,[17] E.Sanchez,[26] M.P.Sanders,[31] M.E.Sarakinos,[21] C.Schäfer,[1] V.Schegelsky,[37] S.Schmidt-Kaerst,[1] D.Schmitz,[1] N.Scholz,[48] H.Schopper,[49] D.J.Schotanus,[31] J.Schwenke,[1] G.Schwering,[1] C.Sciacca,[29] D.Sciarrino,[19] L.Servoli,[33] S.Shevchenko,[32] N.Shivarov,[41] V.Shoutko,[28] J.Shukla,[24] E.Shumilov,[28] A.Shvorob,[32] T.Siedenburg,[1] D.Son,[42] B.Smith,[15] P.Spillantini,[16] M.Steuer,[15] D.P.Stickland,[35] A.Stone,[7] H.Stone,[35] B.Stoyanov,[41] A.Straessner,[1] K.Sudhakar,[11] G.Sultanov,[18] L.Z.Sun,[20] H.Suter,[48] J.D.Swain,[18] Z.Szillasi,[43,¶] X.W.Tang,[8] L.Tauscher,[6] L.Taylor,[12] C.Timmermans,[31] Samuel C.C.Ting,[15] S.M.Ting,[15] S.C.Tonwar,[11] J.Tóth,[14] C.Tully,[35] K.L.Tung,[8] Y.Uchida,[15] J.Ulbricht,[48] E.Valente,[36] G.Vesztergombi,[14] I.Vetlitsky,[28] G.Viertel,[48] S.Villa,[12] M.Vivargent,[4] S.Vlachos,[6] H.Vogel,[34] H.Vogt,[47] I.Vorobiev,[17,28] A.A.Vorobyov,[37] A.Vorvolakos,[30] M.Wadhwa,[6] W.Wallraff,[1] J.C.Wang,[15] X.L.Wang,[20] Z.M.Wang,[20] A.Weber,[1] S.X.Wu,[15] S.Wynhoff,[1] Z.Z.Xu,[20] B.Z.Yang,[20] C.G.Yang,[8] H.J.Yang,[8] M.Yang,[8] J.B.Ye,[20] S.C.Yeh,[51] J.M.You,[34] An.Zalite,[37] Yu.Zalite,[37] P.Zemp,[48] Y.Zeng,[1] Z.P.Zhang,[20] G.Y.Zhu,[8] R.Y.Zhu,[32] A.Zichichi,[10,17,18] F.Ziegler,[47] G.Zilizi.[43,¶]

1 I. Physikalisches Institut, RWTH, D-52056 Aachen, FRG[§]
III. Physikalisches Institut, RWTH, D-52056 Aachen, FRG[§]
2 National Institute for High Energy Physics, NIKHEF, and University of Amsterdam, NL-1009 DB Amsterdam, The Netherlands
3 University of Michigan, Ann Arbor, MI 48109, USA
4 Laboratoire d'Annecy-le-Vieux de Physique des Particules, LAPP,IN2P3-CNRS, BP 110, F-74941 Annecy-le-Vieux CEDEX, France
5 Johns Hopkins University, Baltimore, MD 21218, USA
6 Institute of Physics, University of Basel, CH-4056 Basel, Switzerland
7 Louisiana State University, Baton Rouge, LA 70803, USA
8 Institute of High Energy Physics, IHEP, 100039 Beijing, China[△]
9 Humboldt University, D-10099 Berlin, FRG[§]
10 University of Bologna and INFN-Sezione di Bologna, I-40126 Bologna, Italy
11 Tata Institute of Fundamental Research, Bombay 400 005, India
12 Northeastern University, Boston, MA 02115, USA
13 Institute of Atomic Physics and University of Bucharest, R-76900 Bucharest, Romania
14 Central Research Institute for Physics of the Hungarian Academy of Sciences, H-1525 Budapest 114, Hungary[‡]
15 Massachusetts Institute of Technology, Cambridge, MA 02139, USA
16 INFN Sezione di Firenze and University of Florence, I-50125 Florence, Italy
17 European Laboratory for Particle Physics, CERN, CH-1211 Geneva 23, Switzerland
18 World Laboratory, FBLJA Project, CH-1211 Geneva 23, Switzerland
19 University of Geneva, CH-1211 Geneva 4, Switzerland
20 Chinese University of Science and Technology, USTC, Hefei, Anhui 230 029, China[△]
21 SEFT, Research Institute for High Energy Physics, P.O. Box 9, SF-00014 Helsinki, Finland
22 University of Lausanne, CH-1015 Lausanne, Switzerland
23 INFN-Sezione di Lecce and Universitá Degli Studi di Lecce, I-73100 Lecce, Italy
24 Los Alamos National Laboratory, Los Alamos, NM 87544, USA
25 Institut de Physique Nucléaire de Lyon, IN2P3-CNRS,Université Claude Bernard, F-69622 Villeurbanne, France
26 Centro de Investigaciones Energéticas, Medioambientales y Tecnologícas, CIEMAT, E-28040 Madrid, Spain♭
27 INFN-Sezione di Milano, I-20133 Milan, Italy
28 Institute of Theoretical and Experimental Physics, ITEP, Moscow, Russia
29 INFN-Sezione di Napoli and University of Naples, I-80125 Naples, Italy
30 Department of Natural Sciences, University of Cyprus, Nicosia, Cyprus
31 University of Nijmegen and NIKHEF, NL-6525 ED Nijmegen, The Netherlands
32 California Institute of Technology, Pasadena, CA 91125, USA
33 INFN-Sezione di Perugia and Universitá Degli Studi di Perugia, I-06100 Perugia, Italy
34 Carnegie Mellon University, Pittsburgh, PA 15213, USA
35 Princeton University, Princeton, NJ 08544, USA
36 INFN-Sezione di Roma and University of Rome, "La Sapienza", I-00185 Rome, Italy
37 Nuclear Physics Institute, St. Petersburg, Russia
38 University and INFN, Salerno, I-84100 Salerno, Italy
39 University of California, San Diego, CA 92093, USA
40 Dept. de Fisica de Particulas Elementales, Univ. de Santiago, E-15706 Santiago de Compostela, Spain
41 Bulgarian Academy of Sciences, Central Lab. of Mechatronics and Instrumentation, BU-1113 Sofia, Bulgaria
42 Center for High Energy Physics, Adv. Inst. of Sciences and Technology, 305-701 Taejon, Republic of Korea
43 University of Alabama, Tuscaloosa, AL 35486, USA
44 Utrecht University and NIKHEF, NL-3584 CB Utrecht, The Netherlands
45 Purdue University, West Lafayette, IN 47907, USA
46 Paul Scherrer Institut, PSI, CH-5232 Villigen, Switzerland
47 DESY-Institut für Hochenergiephysik, D-15738 Zeuthen, FRG
48 Eidgenössische Technische Hochschule, ETH Zürich, CH-8093 Zürich, Switzerland
49 University of Hamburg, D-22761 Hamburg, FRG
50 National Central University, Chung-Li, Taiwan, China
51 Department of Physics, National Tsing Hua University, Taiwan, China
§ Supported by the German Bundesministerium für Bildung, Wissenschaft, Forschung und Technologie
‡ Supported by the Hungarian OTKA fund under contract numbers T019181, F023259 and T024011.
¶ Also supported by the Hungarian OTKA fund under contract numbers T22238 and T026178.
♭ Supported also by the Comisión Interministerial de Ciencia y Tecnología.
♯ Also supported by CONICET and Universidad Nacional de La Plata, CC 67, 1900 La Plata, Argentina.
♮ Supported by Deutscher Akademischer Austauschdienst.
◇ Also supported by Panjab University, Chandigarh-160014, India.
△ Supported by the National Natural Science Foundation of China.

# References


[1] S.L. Glashow, Nucl. Phys. **22** (1961) 579; S. Weinberg, Phys. Rev. Lett. **19** (1967) 1264; A. Salam, "Elementary Particle Theory", Ed. N. Svartholm, Stockholm, "Almquist and Wiksell" (1968), 367.

[2] M. Consoli and W. Hollik, in "Z Physics at LEP 1", CERN Report CERN 89-08 Vol.1, 7; M. Böhm and W. Hollik, in "Z Physics at LEP 1", CERN Report CERN 89-08 Vol.1, 203.

[3] L3 Collab., B. Adeva *et al.*, Nucl. Instr. and Meth. **A 289** (1990) 35;
M. Acciarri *et al.*, Nucl. Instr. and Meth. **A 351** (1994) 300;
I.C. Brock *et al.*, Nucl. Instr. and Meth. **A 381** (1996) 236;
A. Adam *et al.*, Nucl. Instr. and Meth. **A 383** (1996) 342.

[4] L3 Collab., M. Acciarri *et al.*, Phys. Lett. **B 335** (1994) 542.

[5] L3 Collab., M. Acciarri *et al.*,
Measurement of the Effective Weak Mixing Angle by Jet–Charge Asymmetry in Hadronic Decays of the Z Boson, Submitted to Phys. Lett.

[6] ALEPH Collab., D. Buskulic *et al.*, Phys. Lett. **B 384** (1996) 414.

[7] DELPHI Collab., P. Abreu *et al.*, Z. Phys. **C 65** (1995) 569;
DELPHI Collab., P. Abreu *et al.*, Phys. Lett. **B 332** (1994) 488.

[8] OPAL Collab., R. Akers *et al.*, Z. Phys. **C 67** (1995) 365.

[9] L3 Collab., B. Adeva *et al.*, Phys. Lett. **B 252** (1990) 703.

[10] L3 Collab., B. Adeva *et al.*, Phys. Lett. **B 288** (1992) 395.

[11] T. Sjöstrand, Comp. Phys. Comm. **39** (1986) 347; T. Sjöstrand and M. Bengtsson, Comp. Phys. Comm. **43** (1987) 367.

[12] The L3 detector simulation is based on GEANT Version 3.15. R. Brun *et al.*, "GEANT 3", CERN DD/EE/84-1 (Revised), September 1987. The GHEISHA program (H. Fesefeldt, RWTH Aachen Report PITHA 85/02 (1985)) is used to simulate hadronic interactions.

[13] ALEPH,DELPHI,L3 and OPAL Collaborations, Nucl. Instr. and Meth. **A 378** (1996) 101.

[14] ALEPH,DELPHI,L3,OPAL and SLD Collaborations,
Input Parameters for the LEP/SLD Electroweak Heavy Flavour Results for Summer 1998 Conferences, in preparation.

[15] C. Peterson *et al.*, Phys. Rev. **D 27** (1983) 105.

[16] G. Altarelli *et al.*, Nucl. Phys. **B 208** (1982) 365.

[17] N. Isgur *et al.*, Phys. Rev. **D 39** (1989) 799.

[18] DELCO Collab., W. Bacino *et al.*, Phys. Rev. Lett. **43** (1979) 1073.

[19] MARK III Collab., R.M. Baltrusaitis *et al.*, Phys. Rev. Lett. **54** (1985) 1976.

[20] CLEO Collab., D. Bortoletto *et al.*, Phys. Rev. **D 45** (1992) 21.

[21] The Particle Data Group, C. Caso et al., Eur. Phys. J. **C3** (1998) 1.

[22] D. Bardin *et al.*, Phys. Lett. **B 255** (1991) 290.

[23] D. Abbaneo *et al.*, Eur. Phys. J. **C4** (1998) 185.
S.C. Blyth, L3 Internal note 2181 (1997). [1)]

[1)] L3 Internal Notes are freely available upon request from
The L3 Secretariat, CERN, CH–1211 Geneva 23, Switzerland.
Internet: http://l3www.cern.ch.

| Category ($k$) | $\mu$ | e | $A_k$ |
|---|---|---|---|
| $\mathrm{b} \to \ell^-$ | 62.7 | 74.7 | $A_b$ |
| $\mathrm{b} \to \mathrm{c} \to \ell^+$ | 7.5 | 5.8 | $-A_b$ |
| $\mathrm{b} \to \tau \to \ell^-$ | 0.9 | 1.1 | $A_b$ |
| $\mathrm{b} \to \bar{\mathrm{c}} \to \ell^-$ | 1.1 | 0.6 | $A_b$ |
| $\mathrm{c} \to \ell^+$ | 10.0 | 6.1 | $-A_c$ |
| background | 17.8 | 11.7 | $A_{bkg}$ |

Table 1: Monte Carlo estimates of the composition (%) of the single lepton data sample and the corresponding asymmetry contributions.

| Category | $\mu\mu$ | ee | $\mu$e | $\ell\ell$ |
|---|---|---|---|---|
| $\mathrm{b} \to \ell$, $\mathrm{b} \to \ell$ | 66.0 | 75.6 | 72.6 | 70.3 |
| $\mathrm{b} \to \ell$, $\mathrm{b} \to \mathrm{c} \to \ell$ | 17.4 | 13.6 | 13.9 | 15.3 |
| $\mathrm{b} \to \ell$, $\mathrm{b} \to$ background | 7.2 | 4.8 | 7.9 | 7.2 |
| $\mathrm{b} \to \mathrm{c} \to \ell$, $\mathrm{b} \to$ background | 1.3 | 0.4 | 4.4 | 0.8 |
| $\mathrm{b} \to \mathrm{c} \to \ell$, $\mathrm{b} \to \mathrm{c} \to \ell$ | 0.7 | 0.7 | 0.3 | 0.5 |
| $\mathrm{b} \to$ background, $\mathrm{b} \to$ background | 0.1 | 0.4 | 0.2 | 0.2 |
| $\mathrm{c} \to \ell$, $\mathrm{c} \to \ell$ | 2.4 | 0.4 | 0.7 | 1.3 |
| others | 4.8 | 4.1 | 3.9 | 4.3 |

Table 2: Monte Carlo composition (%) estimates for the dilepton sample. 'Others' refers to misidentified hadrons or leptons from light hadron decays. The $\mathrm{b} \to \ell$ fraction includes $\mathrm{b} \to \tau \to \ell$ and $\mathrm{b} \to \bar{\mathrm{c}} \to \ell$ decays.

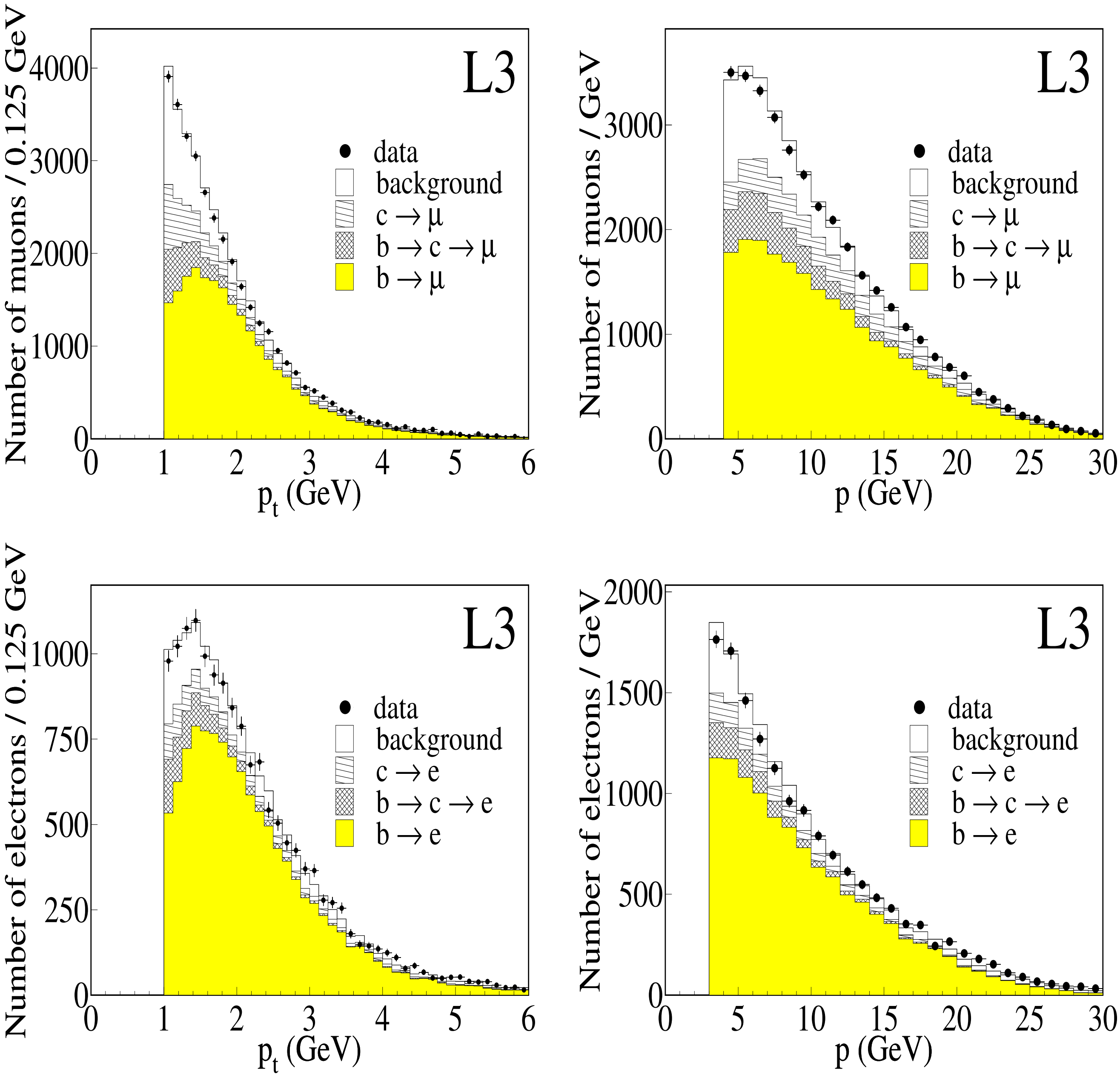


Figure 1: The $p_t$ and $p$ distributions for muons and electrons, with Monte Carlo expectations of contributions from various sources.

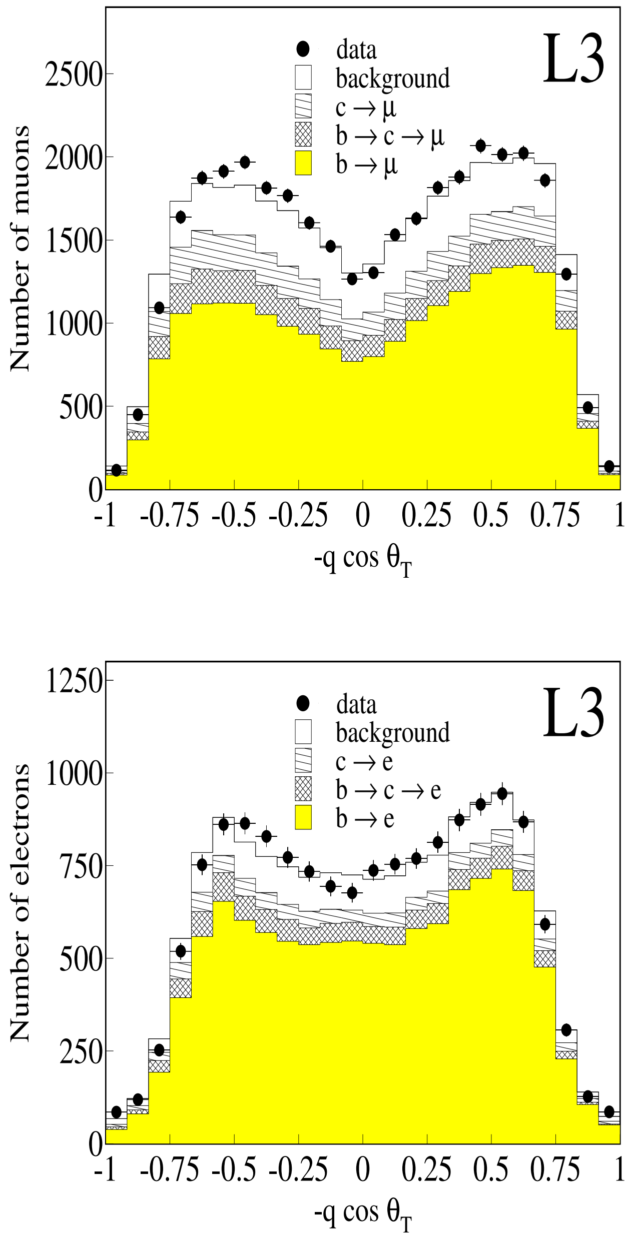


Figure 2: The $-q\cos\theta_{\mathrm{T}}$ distributions for muons and electrons, with Monte Carlo expectations of contributions from various sources.

| Contribution | Value & Variation | $\Delta\chi_{\rm b}$ $\times\,10^2$ | $\Delta A_{\rm FB}^{obs}$ $\times\,10^2$ | $\Delta A_{\rm FB}^{\rm b}$ $\times\,10^2$ |
|---|---|---|---|---|
| $R_b$ | $0.2170 \pm 0.0009$ | $+0.000$ | $-0.008$ | $-0.010$ |
| $R_c$ | $0.1734 \pm 0.0048$ | $+0.001$ | $+0.032$ | $+0.042$ |
| $A_c^{\rm FB}$ | $0.0741 \pm 0.0048$ | $+0.000$ | $+0.051$ | $+0.067$ |
| **Electroweak Parameters** | | **0.001** | **0.061** | **0.079** |
| $\langle x_{\rm E}({\rm b})\rangle$ | $0.7020 \pm 0.0080$ | $+0.000$ | $+0.004$ | $+0.005$ |
| $\langle x_{\rm E}({\rm c})\rangle$ | $0.4840 \pm 0.0080$ | $+0.000$ | $+0.017$ | $+0.023$ |
| ${\rm Br}({\rm b}\to\ell)$ | $0.1050 \pm 0.0050$ | $+0.262$ | $-0.122$ | $-0.092$ |
| ${\rm Br}({\rm b}\to{\rm c}\to\ell^+)$ | $0.0800 \pm 0.0050$ | $-0.291$ | $+0.049$ | $-0.010$ |
| ${\rm Br}({\rm b}\to\bar{\rm c}\to\ell^-)$ | $0.0162 \pm 0.0040$ | $+0.063$ | $-0.017$ | $-0.006$ |
| ${\rm Br}({\rm b}\to\tau\to\ell)$ | $0.0045 \pm 0.0008$ | $+0.000$ | $-0.008$ | $-0.010$ |
| ${\rm Br}({\rm c}\to\ell)$ | $0.0980 \pm 0.0050$ | $+0.003$ | $+0.055$ | $+0.073$ |
| ${\rm Br}({\rm b}\to{\rm J}/\psi\to\ell\ell)$ | $0.0007 \pm 0.0002$ | $+0.000$ | $+0.023$ | $+0.030$ |
| **Fragmentation and Branching Ratios** | | **0.397** | **0.147** | **0.124** |
| ${\rm b}\to\ell$ model | | $-0.030$ | $-0.046$ | $-0.067$ |
| ${\rm c}\to\ell$ model | | $-0.186$ | $+0.116$ | $+0.104$ |
| ${\rm b}\to{\rm D}$ model | | $-0.153$ | $+0.022$ | $-0.010$ |
| **Decay Models** | | **0.243** | **0.127** | **0.125** |
| background fraction | $1.0000 \pm 0.1000$ | $-0.001$ | $+0.049$ | $+0.063$ |
| background asymmetry | $0.0000 \pm 0.0100$ | $+0.000$ | $-0.166$ | $-0.217$ |
| **Background effects** | | **0.001** | **0.173** | **0.226** |
| charge confusion correction | | $-0.097$ | $+0.013$ | $-0.008$ |
| lepton-jet angle smearing | $1^\circ$ | $+0.138$ | $+0.108$ | $+0.145$ |
| lepton momentum smearing | 2% | $+0.011$ | $+0.017$ | $+0.023$ |
| **Detector effects** | | **0.169** | **0.110** | **0.147** |
| $\alpha$,$\beta$,$B$ | $\pm$ 2 % | $+0.132$ | $+0.000$ | $+0.034$ |
| **Mixing specific uncertainties** | | **0.132** | **0.000** | **0.034** |
| **Total Systematic** | | **0.512** | **0.289** | **0.334** |

Table 3: Systematic uncertainties on $\chi_{\rm b}$, $A_{\rm FB}^{obs}$ and $A_{\rm FB}^{\rm b}$ for muons and electrons collected during the 1993-95 peak running periods, $\langle\sqrt{s}\rangle = 91.24$ GeV. The uncertainty totals are obtained from their components by addition in quadrature.

| $\sqrt{s}$ (GeV) | $A_{\rm FB}^{\rm b}$ |
|---|---|
| 89.50 | $0.0611 \pm 0.0293 \pm 0.0043$ |
| 91.26 | $0.0980 \pm 0.0067 \pm 0.0034$ |
| 93.10 | $0.1371 \pm 0.0240 \pm 0.0044$ |

Table 4: $A_{\rm FB}^{\rm b}$ for different centre-of-mass energies after applying QCD corrections. These results are from the full LEP1 data, with statistical and systematic uncertainties provided.

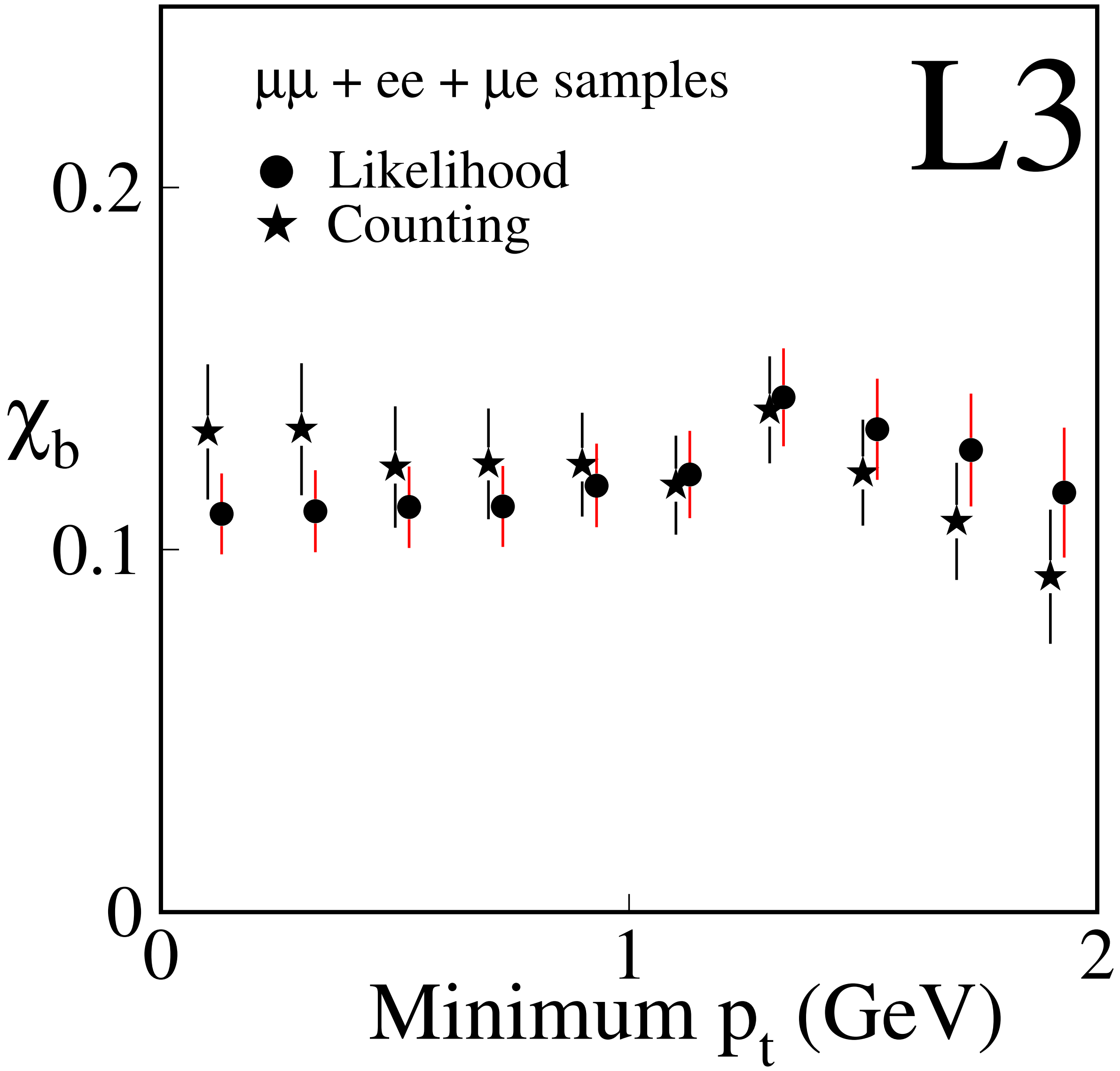


Figure 3: Mixing parameter values as a function of the minimum transverse momentum for the factorized fit method (dots) and a simple counting method (stars). The dots are displaced horizontally for improved visibility.

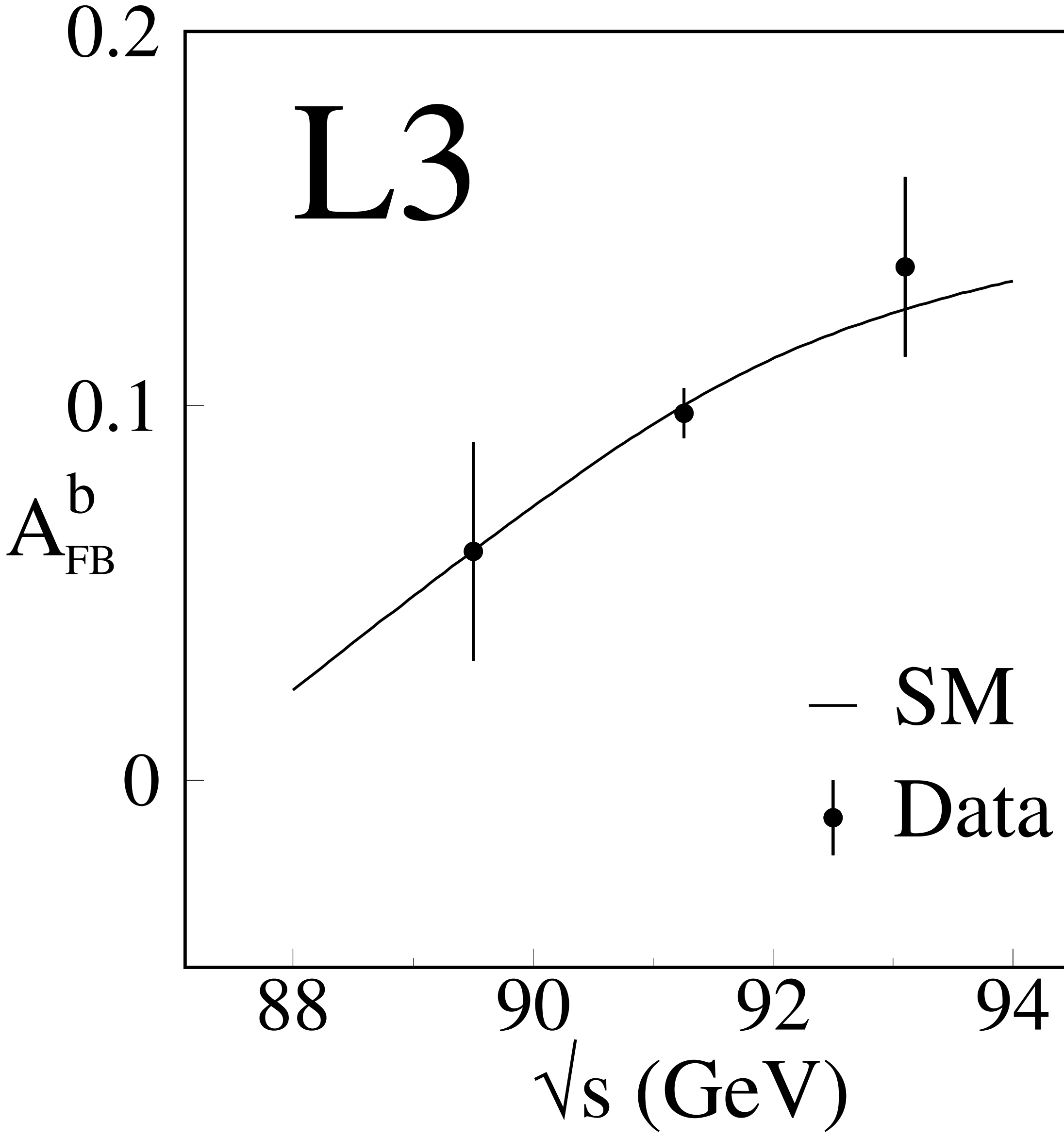


Figure 4: The energy dependence of $A_{\rm FB}^{\rm b}$, after QCD correction, is compared with the Standard Model predictions of ZFITTER with QCD effects removed, corresponding to $\sin^2\bar{\theta}_{\rm W} = 0.2315$.